

Frequency Domain Wave Equation Inversion and Its Application on the Heterogeneous Reservoir Model Data

Zhiyuan Tang^{1,2}

¹ School of information engineer, Hebei GEO University, Hebei province, China

² School of geophysics & information engineering, China University of Petroleum-Beijing, Beijing, China

Correspondence: Zhiyuan Tang, School of information engineer, Hebei GEO University, Hebei province, China.
Tel: 86-182-0254-1220. E-mail: mmg00@163.com

Received: September 26, 2016

Accepted: October 8, 2016

Online Published: December 12, 2016

doi:10.5539/esr.v6n1p55

URL: <http://dx.doi.org/10.5539/esr.v6n1p55>

The research is financed by Doctoral Scientific Research Foundation of China Hebei GEO University.

Abstract

Seismic full waveform inversion seeks to make use of the full information based on full wave field modeling to extract quantitative information from seismograms. Its serious nonlinearity and high dependence on initial velocity model often results in unsatisfactory inversion results in paleo-karsts carbonate reservoir characterized by strong heterogeneity. The paper presents an improved strategy of multi-scale inversion to establish velocity field model of waveform tomography. the forward wave equation algorithm was derived in frequency domain, and then the Matrix formalism for the iterative inverse methods is derived by gradient methods to speed up calculation and to avoid convergence to local minimum value. After massive amount of frequencies tests, the appropriate bandwidth are extracted, and the velocity field calculated at low frequency is used as the input of the high frequency. After the iteration, the accurate velocity field is inverted. Finally, frequency domain wave equation full waveform inversion in mathematical and physical models is conducted in order to verify the inverse program. The method of selecting the inverse frequencies is proved to be effective.

Keywords: seismic wave field modeling, paleo-karsts heterogeneous reservoir, waveform inversion, wave-number cover, velocity model

1. Introduction

Seismic waves bring to the surface information gathered on the physical properties of the earth. Seismic full waveform inversion seeks to make use of the full information based on full wave-field modeling to extract quantitative information from seismograms (Dessa et al. 2007; Operto et al. 2009). Lailly (1983) and Tarantola (1984) recast the migration imaging principle of Claerbout (1976) as a local optimization problem in Born approximation, the aim of which is least squares minimization of the misfit between recorded and modeled data. They show that the gradient of the misfit function along which the perturbation model is searched can be built by cross-correlating the incident wave-field emitted from the source and the back propagated residual wave-fields (Thierry et al. 1999; Brenders et al. 2007). The perturbation model obtained after the first iteration of the local optimization looks like a migrated image obtained by reverse-time migration (Sirgue et al. 2009). One difference is that the seismic wave-field recorded at the receiver is back propagated in reverse time-migration, whereas the data misfit is back propagated in the waveform inversion (Robertson et al. 2007; Vigh et al. 2008). When added to the initial velocity, the velocity perturbations lead to an updated velocity model, which is used as a starting model for the next iteration of minimizing the misfit function. After the iteration, the accurate velocity field is inverted. The key factors that influence Wave equation inversion results are effective and efficient forward modeling (Sirgue et al. 2008), the gradient (Sheng et al. 2006) and Hessian matrix (BenHadjAli et al. 2008) calculation algorithm.

Carbonate reservoir is widely developed in China Tarim basin, where a large number of oil fields are discovered in the paleo-karsts Ordovician limestone reservoir (Peng et al. 2008; Sun et al. 2011). The storage spaces for the carbonate reservoir in this area are mostly secondary dissolution caves and characterized by strong heterogeneity (Zhang et al. 2008; Zeng et al. 2011; Yang et al. 2012). How to accurately image these dissolved caves plays a

key role in exploiting the reservoir and reserve estimation (Zhang et al. 2011; Tang et al. 2012). Due to low signal to noise ratio, the accuracy of velocity model used in pre-stack migration is very important. Considering the question mentioned above, seismic full waveform inversion is introduced seeks to make use of the information based on full wave field modeling to extract quantitative information from seismograms. The paper presents an improved strategy of multi-scale inversion to establish accuracy depth migration velocity field as an initial input model of waveform tomography, so that decrease the serious nonlinearity. The velocity field calculated at low frequency is used as the input of the high frequency, the accurate velocity field is inverted after the iteration. In the application of the frequency domain waveform inversion approach, we use seismic data from mathematic model and a caved physical model which is supplied by CNPC (China National Petroleum Corporation) key laboratory. several critical processes that contribute to the success of the method were tested here like, the matching of amplitudes between real and synthetic data, the selection of sequence of frequencies in the inversion, and the relationship between inversion velocity model and wave number reconstruction.

2. Waveform inversion method

The correction of full waveform inversion relies on the accuracy of its forward modeling wave equation. It can get good result only when forward modeling is approximate with actual process of wave propagate. The forward wave equation is derived in frequency domain. The pressure is computed using a staggered-grid, explicit finite-difference method. The Matrix formalism for the iterative inverse methods is derived which include gradient and Gauss Newton methods to speed up calculation and to avoid convergence to local minimum value. After massive amount of frequencies tests, the appropriate bandwidth are extracted, and the velocity field calculated at low frequency is used as the input of the high frequency. After the iteration, the accurate velocity field is inverted. Here we deal with a 2D acoustic wave equation written in the frequency domain as,

$$\frac{\partial}{\partial x} \left(\frac{1}{\rho(x,z)} \frac{\partial p(x,z,\omega)}{\partial x} \right) + \frac{\partial}{\partial z} \left(\frac{1}{\rho(x,z)} \frac{\partial p(x,z,\omega)}{\partial z} \right) + \frac{\omega^2}{K(x,z)} p(x,z,\omega) = -g(x,z,\omega) \tag{1}$$

where ρ is the density, K the complex bulk modulus, ω the frequency, p the pressure field and g is the source.

In the frequency domain, the wave equation can be compactly written as

$$B(X,\omega)P(X,\omega) = G(X,\omega) \tag{2}$$

where B is the so called impedance matrix. Solving equation (2) can be performed through LU factorization of B (Virieux et al. 2009).

We define the misfit vector $\delta d = d_{obs} - d_{cal}(m)$ by the difference at the receiver positions between the recorded seismic data d_{obs} and the modeled one $d_{cal}(m)$. The misfit vector $C(m)$ referred to as the misfit function.

We use the least square norm which is easier to manipulate from a mathematical point of view is given by

$$C(m) = \frac{1}{2} \|\delta d\|^2 = \frac{1}{2} \delta d^\dagger \delta d \tag{3}$$

where \dagger denotes the complex conjugate, m the model parameters.

The gradient of the misfit function in equation (3) with respect to slowness perturbation is computed by the zero-lag correlation between the forward-propagated wavefields and the back-projected wavefield residuals,

$$\nabla C = \Re \left[P^\dagger \frac{\partial B^\dagger}{\partial m^\dagger} B^{-1\dagger} \delta d \right] \tag{4}$$

The velocity model is iteratively updated along the conjugate directions defined by

$$X_{k+1} = X_k - \alpha_k H_k \nabla f_k \tag{5}$$

where iterations $k=1,2,\dots,k_{max}$, α_k is the step length, which is computed by a line search that ensures sufficient decrease of f_k , and H_k is an approximation of the inverse of the Hessian (Brossier et al. 2009). At each iteration, one forward propagation and one back projection are needed for computing the gradient direction.

3. Application 1. Mathematic Model

China western carbonate reservoir is characterized by deep buried (greater than 5 km), complex surface condition and weak inner reflection. The core analyses indicate that the matrix porosity in carbonate reservoir is extremely low (<2%). The storage spaces are dissolution pores and fractures which are dominated by dissolution caves and fractures characterized by strong heterogeneity. It has obvious velocity difference between the matrix carbonate and the caved reservoir. In order to study this type of reservoir, We designed a 2D heterogeneous reservoir mathematic model parameters shown in figure 1. It is 9 km in length, and 3 km in depth. The grid size is set to 30 m * 30 m. There are two caves in this model. The large one's diameter is 200 m and the filled material velocity is 2200 m/s. while, the small one's diameter is 60 m, and the filled material velocity is 1800 m/s. The model background velocity is 2000 m/s.

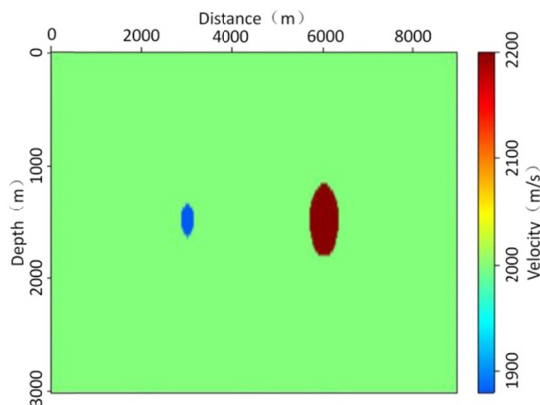


Figure 1. Mathematic model parameters

Note. There are two caves of different sizes and filled materials in the model. The large one with high velocity and the small one with low velocity.

The seismic acquisition system was designed as follow, both shot and receivers were put on the earth's surface, the shot start from (0 m, 0 m) , a total of 290 shots were collected with shot interval 30 m from left to right. The receivers were put both sides of the shot with receiver interval 10 m, the maximum number of receivers of a shot gather is 500. The source used for forward modeling is a Rick wavelet with 10Hz domain frequency. The synthetic data was made in frequency domain and translate into time domain by inverse Fourier transform, as shown in figure 2.

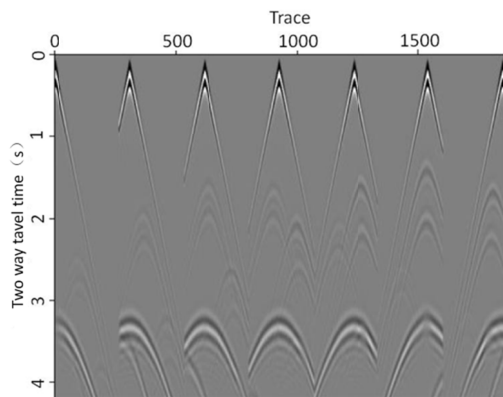


Figure 2. The synthetic shot gathers of caved Mathematic model of figure 2 (only 7 shot gathers show here)

Figure 3 shows the inversion results of two different initial velocity models after 20 times iteration. The inversion frequency range from 1Hz to 30Hz, with frequency interval of 0.5Hz, a total of 59 frequency points were inverted in each iteration. The low frequency inversion result is the input initial velocity model of high frequency. It shows that in the inversion of background velocity model case, the caves are bigger than actual

and we can not get the exact velocity in the cave (Figure 3a). This problem can be solved by using actual velocity model as initial velocity model (Figure 3b).

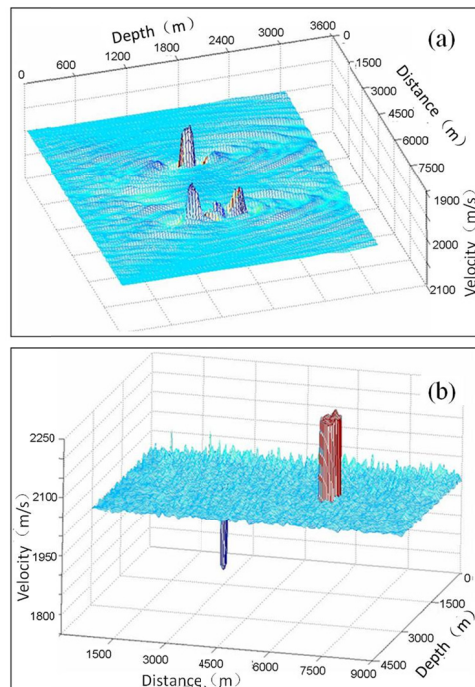


Figure 3. Inversion results of, a) background velocity model, and b) actual velocity model

Note. A total of 59 frequencies range from 1Hz to 30Hz , each frequency was inverted after 20 times iteration.

The wave equation inversion results were theoretical analysis by small velocity disturbance model here. The relationship between velocity model inversion results and wave number reconstruction had already been discussed by Wu, et al. (1987), from which velocity disturbance model can be reconstructed from scattering wave field wave number spectrum. Figure 4 is the comparison of the big cave amplitude spectral between real velocity disturbance model and inversion results. Logarithm amplitude spectral analysis is used to get more detail information. It can be seen that the inversion results match the real velocity disturbance model, most of the wave number had been recovered in this study. Influenced by the reflection seismic acquisition system of both source and reservoirs are put on the earth surface, the wave number recover result in distance direction is better than depth direction. The slightly disturbance velocity in the picture is caused by lack of low wave number component in both wave equation forward modeling and inversion.

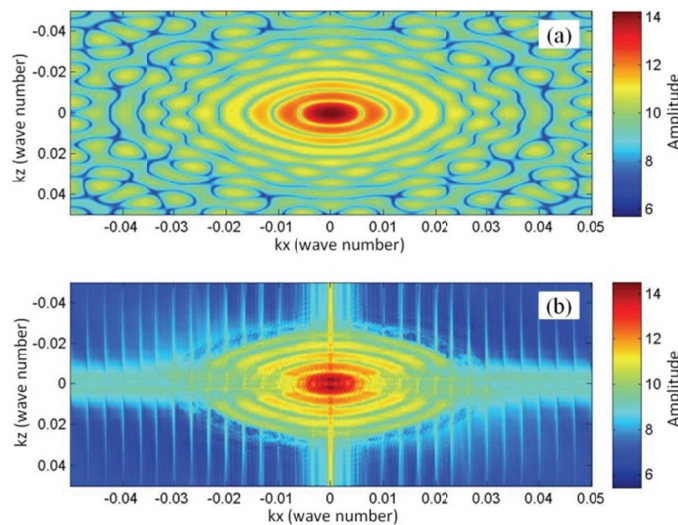


Figure 4. The logarithm of disturbance amplitude spectrum of, a) real velocity model, and b) inversion result

4. Application 2. Caved Physical Model

A caved physical model was made and seismic data was collected by CNPC key lab in this study. as is shown in figure 5. The model was placed in a tank filled with water. On seismic data acquisition, both source and receiver probe are set on water surface. The source probe produces ultrasonic wave which travel through the water and model layers. In this way, sets of reflection will be produced and back to the receiver. This method of seismic data collection system is similar to marine seismic exploration. The model has two layers named layer 1 (white, mixture materials of epoxy resin and silicone rubber) and layer 2 (yellow, epoxy resin).



Figure 5. The seismic data acquisition system in CNPC key lab

Note. The physical model was put in water and The seismic data collection method is similar to marine seismic exploration.

The velocity parameters of the physical model are designed as shown in figure 6. The distance between the model upper surface and the water surface is 1400m. The model is 9000m in length, 3000m in depth, and the grid size is 10 m * 10 m. There are 6 caves in layer 2 which filled with different materials, namely, gas (340m/s), water (1490m/s), oil (1280m/s), silastic (540m/s), mixed material 1 (1020m/s), and mixed material 2 (2016m/s). The diameters of each cave is 30m. The physical model simulation proportion is 1/10000.

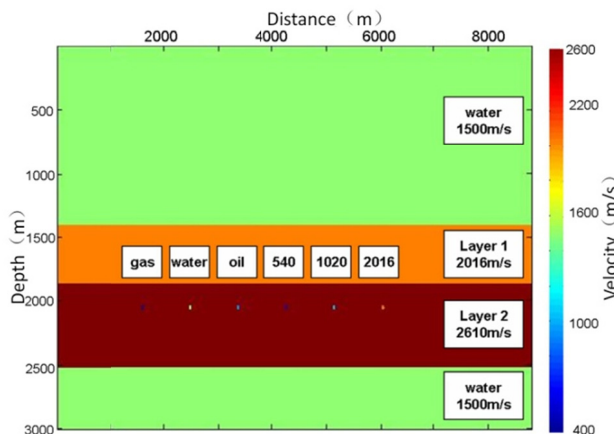


Figure 6. The caved physical model velocity parameters

Note. There are six caves in the layer 2. each cave with the diameter of 30 m, and was filled by different material (the Simulation proportion: 1/10000)

The seismic acquisition system was designed as follow, the first shot start from (0 m, 0 m), with the shot interval 40 m, a total of 160 shots were collected from left to right. Each shot with 120 receivers put on the right of the source, the receiver interval is 20 m, and the minimum offset is 160 m. The domain frequency in target layer is about 25Hz. Figure 7 shows the comparison between seismic shot gathers and synthetic shot gathers we used in

the inversion. The wave equation forward modeling use Rick wavelet with the frequency range from 1Hz to 60Hz, frequency interval of 0.3Hz. The synthetic data was made in frequency domain and translate into time domain by inverse Fourier transform. It shows that the reflection of gas hole can clearly be seen both in seismic acquisition gather and synthetic gather, the multiple waves can not be see in synthetic shot gather due to the PML (perfect match layer) boundary was put here. Restricted lack of high frequency in wave equation forward modeling make the synthetic data has low resolution compared with the seismic acquisition data.

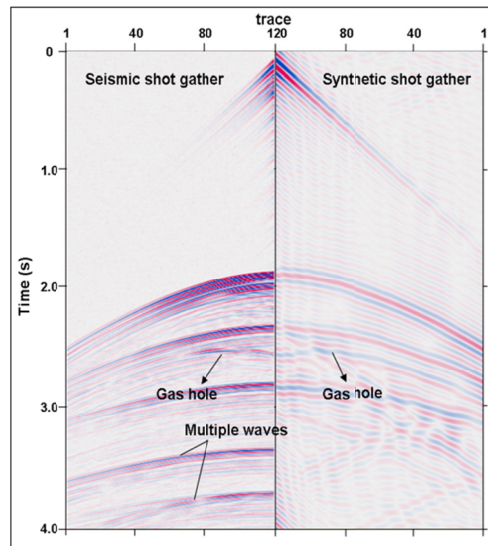


Figure 7. The comparison between seismic shot gathers and synthetic shot gathers

Note. The reflection of gas hole can clearly be seen here, the multiple waves can not be see in synthetic shot gather due to the PML (perfect match layer) boundary was put here.

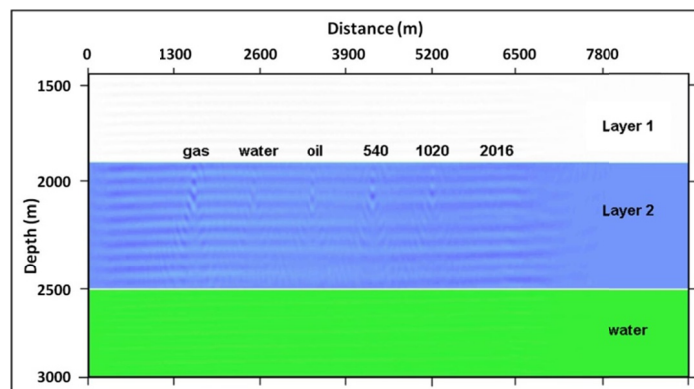


Figure 8. Inversion results of caved physical mode

Note. The initial velocity model is the background velocity, and a total of 10 frequencies were inverted after 20 times iteration.

Figure 8 is the result of full waveform inversion after 20 times iteration. The input initial velocity model is model background velocity, The inversion frequency range from 5Hz to 50Hz, with frequency interval of 5Hz, a total of 10 frequency points were inverted in each iteration. It shows the caves features of physical model and the size of each cave has close relationship with the fluid details in the caves. Some parallel lines can be seen in layer1 and layer2, which may be affected by the layered casting process in model production to meet the cooling demands of epoxy resin solidifying system.

5. Conclusions

The frequency domain wave equation inversion renews the velocity model by cross correlating the incident wave-field from the seismic acquisition data and the back propagated residual wave-fields. The strategy of

multi-scale inversion by selecting the inverse frequencies is proven to be effective for the strong heterogeneity reservoir, suggested by the application of mathematic and physical model data.

Acknowledgments

Identify grants or other financial support (and the source, if appropriate) for your study; do not precede grant numbers by No. or #. Next, acknowledge colleagues who assisted in conducting the study or critiquing the manuscript. Do not acknowledge the persons routinely involved in the review and acceptance of manuscripts [≠] peer reviewers or editors, associate editors, and consulting editors of the journal in which the article is to appear. In this paragraph, also explain any special agreements concerning authorship, such as if authors contributed equally to the study. End this paragraph with thanks for personal assistance, such as in manuscript preparation.

References

- BenHadjAli, H., Operto, S., & Virieux, J. (2008). Velocity model building by 3D frequency domain full waveform inversion of wide aperture seismic data [J]. *Geophysics*, 73(5), VE101–VE117.
- Brenders, A., & Pratt, R. (2007). Efficient waveform tomography for lithosphere imaging: Implications for realistic 2D acquisition geometries and low frequency data [J]. *Geophysical Journal International*, 168, 152-170.
- Brossier, R., Operto, S., & Virieux, J. (2009). Seismic imaging of complex structures by 2D elastic frequency-domain full-waveform inversion [J]. *Geophysics*, 74(6), WCC105-WCC118.
- Claerbout, J. (1976). *Fundamentals of geophysical data processing [M]*. McGraw-Hill Book Co., Inc, 1976.
- Dessa, J., & Pascal, G. (2003). Combined travel time and frequency-domain seismic waveform inversion: A case study on multi-offset ultrasonic data [J]. *Geophysical Journal International*, 154, 117-133.
- Lailly (1983). Conference on Inverse Scattering, Theory and Application [C], Society for Industrial and Applied Mathematics, *Expanded Abstracts*, 190, 206-220.
- Operto, S., Virieux, J., Ribodetti, A., et al. (2009). Finite-difference frequency-domain modeling of viscous acoustic wave propagation in two dimensional tilted transversely isotropic media [J]. *Geophysics*, 74(5), T75-T95.
- Peng, Z., Li, Y., Wu, S., et al. (2008). Discriminating gas and water using multi-angle extended elastic impedance inversion in carbonate reservoirs [J]. *Geophysics (in Chinese)*, 51(3), 881-885.
- Robertson, J., Bednar, B., Blanch, J., et al. (2007). Introduction to the supplement on seismic modeling with applications to acquisition, processing and interpretation [J]. *Geophysics*, 72(5), M1-M4.
- Sheng, J., Leeds, A., Buddensiek, M., et al. (2006). Early arrival waveform tomography on near surface refraction data [J]. *Geophysics*, 71(4), U47-U57.
- Sirgue, L., Barkved, O., Gestel, J., et al. (2009). *2D waveform inversion on Valhall wide azimuth OBS [C]*. 71st Conference & Technical Exhibition EAGE Extended Abstracts, U038- U042.
- Sirgue, L., Etgen, J., & Albertin, U. (2008). *3D frequency domain waveform inversion using time domain finite difference methods [C]*. 70th Conference & Technical Exhibition EAGE Extended Abstracts, F022.
- Sun, S., Zhou, X., Li, Y., Wang, H., et al. (2011). *Fluid Identification of Caved Carbonate Reservoir Based on Prestack Inversion [C]*. 73rd EAGE Conference & Exhibition, 2011.
- Tang, Z., Sun, Z., Wei, J., et al. (2012). Analysis on impact factors of quantitative volume estimation for karst-cave based on physical modeling data [J]. *Geophysical prospecting for petroleum*, 51(5), 431-439.
- Tarantola, A. (1984). Inversion of seismic reflection data in the acoustic approximation [J]. *Geophysics*, 49, 1259-1266.
- Thierry, P., Operto, S., & Lambaré, G. (1999). Fast 2D ray-Born inversion/migration in complex media [J]. *Geophysics*, 64(1), 162-181.
- Vigh, D., & Starr, E. (2008). 3D plane wave full waveform inversion [J]. *Geophysics*, 73(5), VE135–VE144.
- Virieux, J., & Operto, S. (2009). An overview of full-waveform inversion in exploration geophysics [J]. *Geophysics*, 74(6), 127-152.
- Wu, R., & Toksöz, M. (1987). Diffraction tomography and multisource holography applied to seismic imaging. *Geophysics*, 52(1), 11-25
- Yang, P., Sun, S., Liu, Y., et al. (2012). Origin and architecture of fractured-cavernous carbonate reservoirs and

their influences on seismic amplitudes [J]. *The Leading Edge*, 31,140-150.

Zeng, H., Wang, G., Janson, X., et al. (2011). Characterizing seismic bright spots in deeply buried, Ordovician Paleokarst strata, Central Tabei uplift, Tarim Basin, Western China [J]. *Geophysics*, 76(4), 127-137.

Zhang, H., Zheng, J., Yang, D., et al. (2008). Prediction of paleo-karst reservoir in the southeastern slope of Tazhong area in Tarim basin using seismic techniques [J]. *Acta Petrolei Sinica*, 29(1), 69-74.

Zhang, Y., Sun, Z., Yang, H., et al. (2011). Pre-stack inversion for caved carbonate reservoir prediction: a case study from China Tarin basin [J]. *Petroleum science*, 8(4), 415-421.

Copyrights

Copyright for this article is retained by the author(s), with first publication rights granted to the journal.

This is an open-access article distributed under the terms and conditions of the Creative Commons Attribution license (<http://creativecommons.org/licenses/by/4.0/>).